

(17)

Spontaneous broken symmetry in nuclei is, as a rule associated with the presence of rotational bands, as already found in the case of quadrupole deformed nuclei. Consequently, one expects in nuclei with $\Delta \neq 0$ rotational bands, in which particle number plays the role of angular momentum. That is pairing rotational bands. In what follow we will discuss the structure of H_{pert} and single out the term responsible for restoring gauge invariance to the BCS mean field solution, and thus, give rise to pairing rotation.

Spontaneously broken symmetry in nuclei is, as a rule associated with the presence of rotational bands, as already exemplified by the case of quadrupole deformed nuclei.

~~In gauge space, the different orientations in gauge space have the same energy, as no restoring force is associated with such a process.~~

~~[Instead of proceeding as in the case of rotations in 3D-space], we will extract the component of H_{fluct} , responsible to generate rotation in gauge space.~~

~~Consequently, one expects rotational bands in which particle number plays the role of angular momentum. That is pairing rotational bands.~~

In terms of quaniparticles, H_{fluct} can be expressed as

$$H_{\text{fluct}} = H_p' + H_p'' + C \quad (0.1.89)$$

(0.1.72)

where

$$H_p' = -\frac{G}{4} \left(\sum_{v>0} (U_v^2 - V_v^2) (\Gamma_v^+ + \Gamma_v^-) \right)^2 \quad (0.1.90)$$

(0.1.73)

and

$$H_p'' = \frac{G}{4} \left(\sum_{v>0} (\Gamma_v^+ - \Gamma_v^-) \right)^2, \quad (0.1.91)$$

(0.1.73)

with

$$\Gamma_v^\pm = \alpha_v^\pm \bar{\alpha}_v^\pm. \quad (0.1.92)$$

(0.1.74)

The term C stands for constant terms, as well as for terms proportional to the number of quaniparticles, ~~which~~ which consequently vanish when acting on $\langle BCS \rangle$.

The term H_p gives rise two-quasiparticle pairing vibrations with energies $\gtrsim 2\Delta$. It can be shown that it is the term H_p'' which restores gauge invariance*,) (98)

$$[H_{MF} + H_p'', \hat{N}] = 0 \quad (O.1.93)$$

(O.1.75)

We now diagonalize $H_{MF} + H_p''$ in the quasi-particle RPA (QRPA),

$$[H_{MF} + H_p'', \Gamma_n^+] = \hbar\omega_n \Gamma_n^+, \quad [\Gamma_n^+, \Gamma_{n'}^+] = \delta(n, n'), \quad (O.1.94)$$

where

$$\Gamma_n^+ = \sum_v (a_{nv} \Gamma_v^+ + b_{nv} \Gamma_v^-), \quad \Gamma_v^+ = \alpha_v^+ \alpha_v^- \quad (O.1.95)$$

(O.1.76)
(O.1.94)

is the creation operator of the n th vibrational mode. In the case of the $n=1$, lowest energy root, it can be written as

$$\Gamma_1^+ = \frac{\Lambda_1''}{2\Delta} (\hat{N} - N_0), \quad (O.1.78)$$

where \hat{N} is the particle number operator written in terms of Γ_v^+ and Γ_v^- , and Λ_1'' is the strength of the quasiparticle-mode coupling. The prefactor is the zero point fluctuation (ZPF) of the mode, that is (Eq. O.1.10)

$$\sqrt{\frac{\hbar\omega_1''}{2C_1''}} = \sqrt{\frac{\hbar^2}{2D_1'' \hbar\omega_1''}} \quad (O.1.79)$$

(O.1.97)

*) For detail see Brühad Broglie (2005)

Because the frequency $\omega_1'' = 0$, the associated ZPF diverge ($\Lambda_1'' \sim (\hbar\omega_1'')^{-1/2}$). It can be shown that this is because $C_1'' \rightarrow 0$, while D_1'' remains finite. (18) (19)

In fact,

$$\frac{D_1''}{\hbar^2} = \frac{2\Delta^2}{\Lambda_1''^2 \hbar \omega_1''} = 4 \sum_{v>0} \frac{U_v^2 V_v^2}{2E_v}. \quad (O.1.98)$$

Because a rigid rotation in gauge space can be generated by a series of infinitesimal operations of type $g(\delta\phi) = e^{i(N-N_0)\delta\phi}$, the one phonon state $|1''\rangle = |\Gamma_1^+ 10''\rangle$, is obtained from rotations in gauge space of divergent amplitude. That is, fluctuations of ϕ over the whole $0-2\pi$ range. By proper inclusion of these fluctuations one can restore gauge invariance violated by $|BCS\rangle_K$. The resulting state: (O.1.99)

$$|N\rangle \sim \int_0^{2\pi} d\phi e^{-iN_0\phi} |BCS(\phi)\rangle_K \sim \left(\sum_{v>0} C'_v P_v^+ \right)^{1/2} |10\rangle_F$$

~~means~~ have a definite number of particles and constitute the members of a pairing rotational band, [For example the that represented by the ground state of the $^{100}_{50}\text{Sn}$ -isotopes, open shell, superfluid nuclei.]

Making use of a simplified model (single γ -shell*) it can be shown that

~~Brown ad Brueckle App. H~~

~~consequently approx~~

(20)

the energy of these states can be written
as (App. O.A) ← App C Auger Bohr contrs. (see App H Brink+Brueck)

$$E_N = \lambda(N - N_0) + \frac{G}{4}(N - N_0)^2, \quad (O.1.100)$$

where

$$\frac{G}{4} = \frac{\hbar^2}{2D''} \cdot \quad (O.1.101)$$

An example of pairing rotational bands is provided by the ground state of the single open closed shell superfluid isotopes of the $^{16}_{50}\text{Sn}$ -isotopes (Fig. O.1.15) FIG. 9
paper PRC 87, $N_0 = 68$ having been used in the solution of the BCS number equation (O.1.72). Theory provides an overall account of the experimental findings.

Making use of the BCS pair transfer amplitudes,

$$\langle B_{CS} | P^+ | B_{CS} \rangle = U, V, \quad (O.1.102)$$

in combination with a reaction software and of global optical parameters, one can account for the absolute value of the pair transfer differential cross section, within experimental errors (Fig. 6.4.1).

The fact that projecting out the different Sn-isotopes from the intrinsic BCS state describing ^{118}Sn one obtains a quantitative description of observations carried out with the help of the specific probe of pairing correlations (cooper pair transfer), testifies to the fact that pairing rotational bands can be considered elementary modes of nuclear excitation, emergent properties of spontaneous symmetry breaking of

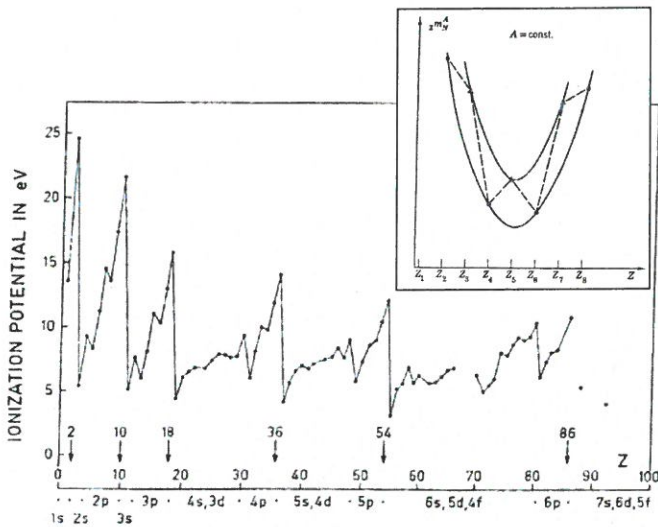
gauge invariance.

(21)

Furthermore, the fact that these results follow the use of QRPA*) in the calculation of the ZPF of the collective solutions of the pairing Hamiltonian indicates the importance of conserving approximations to describe many-body problems in general, and the finite size many-body problem (FSMB) of which the nuclear case represents a paradigmatic example.

to p. 6
HFB manuscript

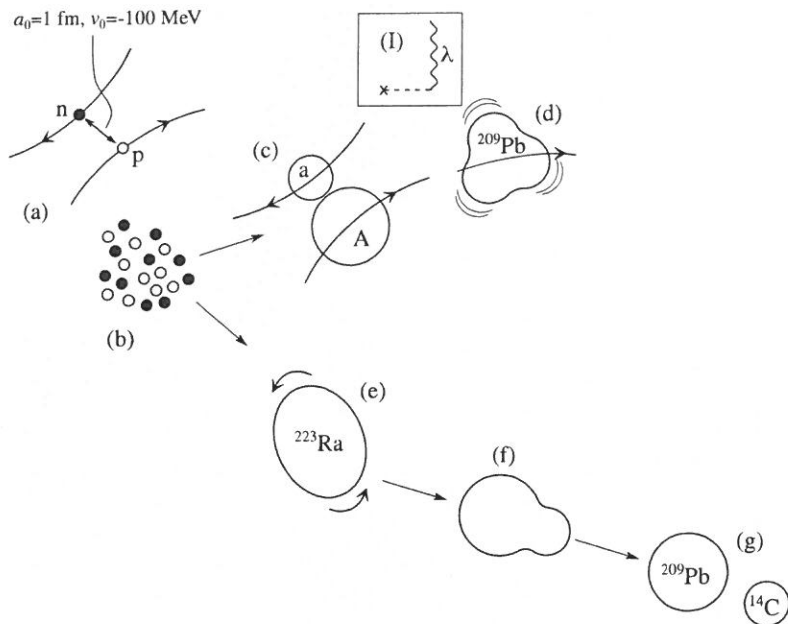
*) Using the Tamm-Dancoff approximation, i.e. setting $Y \equiv 0$ (and thus $\sum X^2 = 1$) in the QRPA approximation does not lead to particle number conservation, in keeping with the fact that the amplitudes Y are closely connected with ZPF.



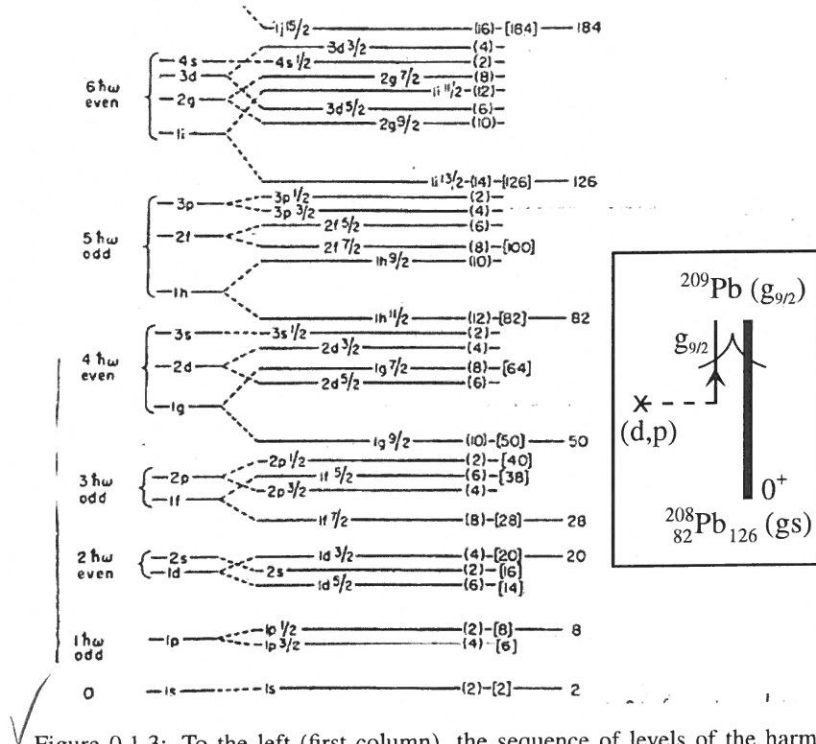
✓ Figure 0.1.1: The values of the atomic ionization potentials. The dots under the abscissa indicate closed shells, corresponding to electron numbers: 2(He), 10(Ne), 18(Ar), 36(Kr), 54(Xe), and 86(Ra). After Bohr and Mottelson (1969). In the inset, masses of nuclei with even A are shown (after Mayer and Jensen (1955)).

the proper interaction leading to realistic Hartree–Fock mean field and collective RPA particle–hole and pairing vibrational modes. As one possible return of such input, nuclear field theory will eventually be able to provide shell model practitioners, friendly and accurate microscopic collective modes of excitation input.

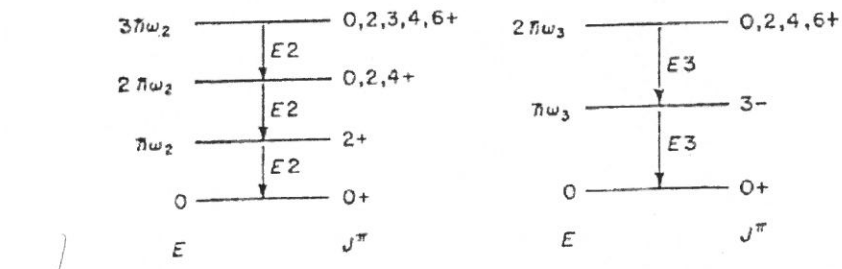
The possible outcome of such collaboration and interplay could be that of being able to coin into few physical concepts the elements needed to accurately describe the atomic nucleus. In other words, carry out calculations which are largely independent of the basis chosen. That is truly predictive theories of structure and reactions, in which the physical content is simple to apprehend and visualize.



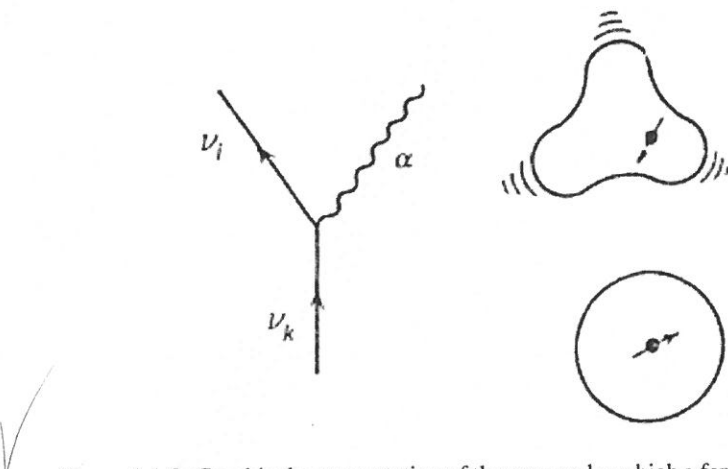
✓ Figure 0.1.2: Emergent properties (collective nuclear models) (a) Nucleon-Nucleon (NN) interaction in a scattering experiment; (b) assembly of a swarm of nucleons condensing into drops of nuclear matter, examples shown in (c) and (e); (c) anelastic heavy ion reaction $a + A \rightarrow a + A^*$ setting the nucleus A into an octupole surface oscillations (d); in inset (I) the time-dependent nuclear plus Coulomb fields associated with the reaction (c) is represented by a cross followed by a dashed line, while the wavy line labeled λ describes the propagation of the surface vibration shown in (d), time running upwards; (e) another possible outcome of nucleon condensation: the (weakly) quadrupole deformed nucleus ^{223}Ra which can rotate as a whole with moment of inertia smaller than the rigid moment of inertia, but much larger than the irrotational one; (f) the surface of a quantal drop fluctuates (zero point fluctuations), with the variety of multipolarities with which the system reacts to time-dependent Coulomb/nuclear external fields (quadrupole ($\lambda = 2$), octupole ($\lambda = 3$), etc.), eventually producing a neck-in (saddle conformation) and the exotic decay $^{223}\text{Ra} \rightarrow ^{209}\text{Pb} + ^{14}\text{C}$ as experimentally observed (g).



✓ Figure 0.1.3: To the left (first column), the sequence of levels of the harmonic oscillator potential labeled with the total oscillator quantum number and parity $\pi = (-1)^N$. The next column shows the splitting of major shell degeneracies obtained using a more realistic potential (Woods-Saxon), the quantum number being the number of radial nodes of the associated single-particle wave functions. The levels shown at the center result when a spin-orbit term is considered the quantum numbers nlj characterizing the states of degeneracy $(2j+1)$ ($j = |l \pm 1/2|$) (After Mayer (1963)). In the inset, a schematic graphical representation of the reaction $^{208}_{82}\text{Pb}_{126}(d, p)^{209}\text{Pb}(\text{gs})$ is shown. A cross followed by a horizontal dashed line represents here the (d, p) field, while a single arrowed line describes the odd nucleon moving in the $g_{9/2}$ orbital above $N = 126$ shell closure drawn as a bold line labeled 0^+ .



✓ Figure 0.1.4: Harmonic quadrupole and octupole liquid drop collective surface vibrational modes.



✓ Figure 0.1.5: Graphical representation of the process by which a fermion, bouncing inelastically off the surface, sets it into vibration. Particles are represented by an arrowed line, while the vibration is shown by a wavy line. The black dot represents a nucleon moving in a spherical mean field of which it excites an octupole vibration after bouncing inelastically off the surface.

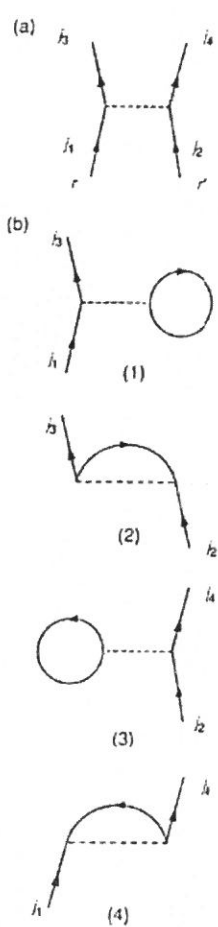


Figure 0.1.6: (a) Scattering of two nucleons through the bare NN -interaction; (b) (1) and (3): Contributions to the (direct) Hartree potential;(2) and (4): contributions to the (exchange) Fock potential.

$$(a) \quad \hat{\alpha} = \sum_{\nu_k \nu_i} \nu_k \nu_i +$$

$$(b)$$

$$(c)$$

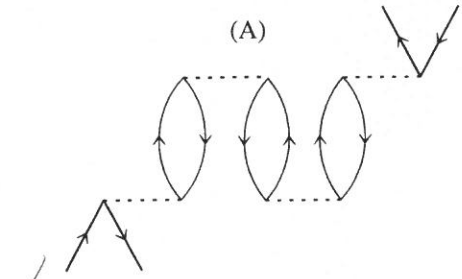


Figure 0.1.7: (A) typical Feynman diagram diagonalizing the NN -interaction $v(|\mathbf{r}-\mathbf{r}'|)$ (horizontal dashed line) in a particle-hole basis provided by the Hartree-Fock solution of v , in the harmonic approximation (RPA). Bubbles going forward in time (inset (b)) are associated with configuration mixing of particle-hole states. Bubbles going backwards in time (inset (c)) are associated with zero point motion (fluctuations ZPF) of the ground state (term $1/2\hbar\omega$ for each degree of freedom in Eq. 0.1.11). The self consistent solution of A is represented by a wavy line (inset (a)), that is a collective mode which can be viewed as a correlated particle hole excitation.

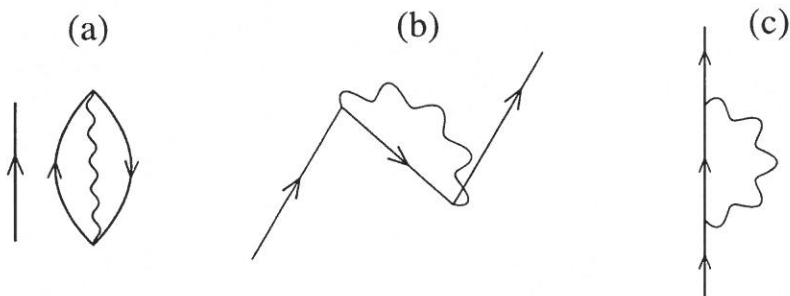


Figure 0.1.8: (a) a nucleon (single arrowed line) moving in presence of the zero point fluctuation of the nuclear ground state associated with a collective surface vibration; (b) Pauli principle leads to a dressing event of the nucleon; (c) time ordering gives rise to the second possible lowest order clothing process (time assumed to run upwards).

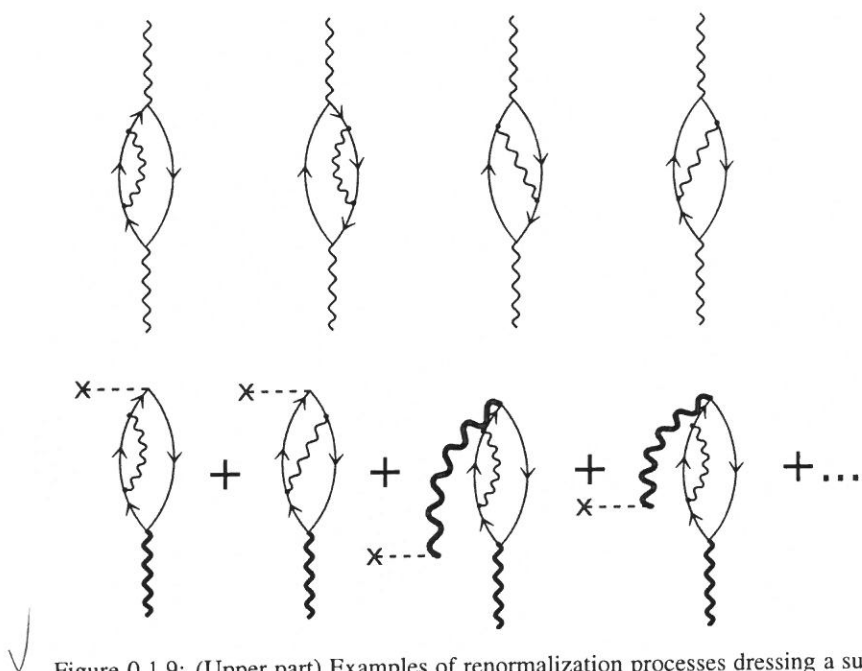


Figure 0.1.9: (Upper part) Examples of renormalization processes dressing a surface collective vibrational state. (Lower part) Intervening with an external electromagnetic field ($E\lambda$: cross followed by dashed horizontal line; bold wavy lines, vibration of multipolarity λ) the $B(E\lambda)$ transition strength can be measured.

$$x_{--} = \sum_k x_{--}^k R + \sum_i x_{--}^i i$$

Fig. 0.1, 41
¹⁰

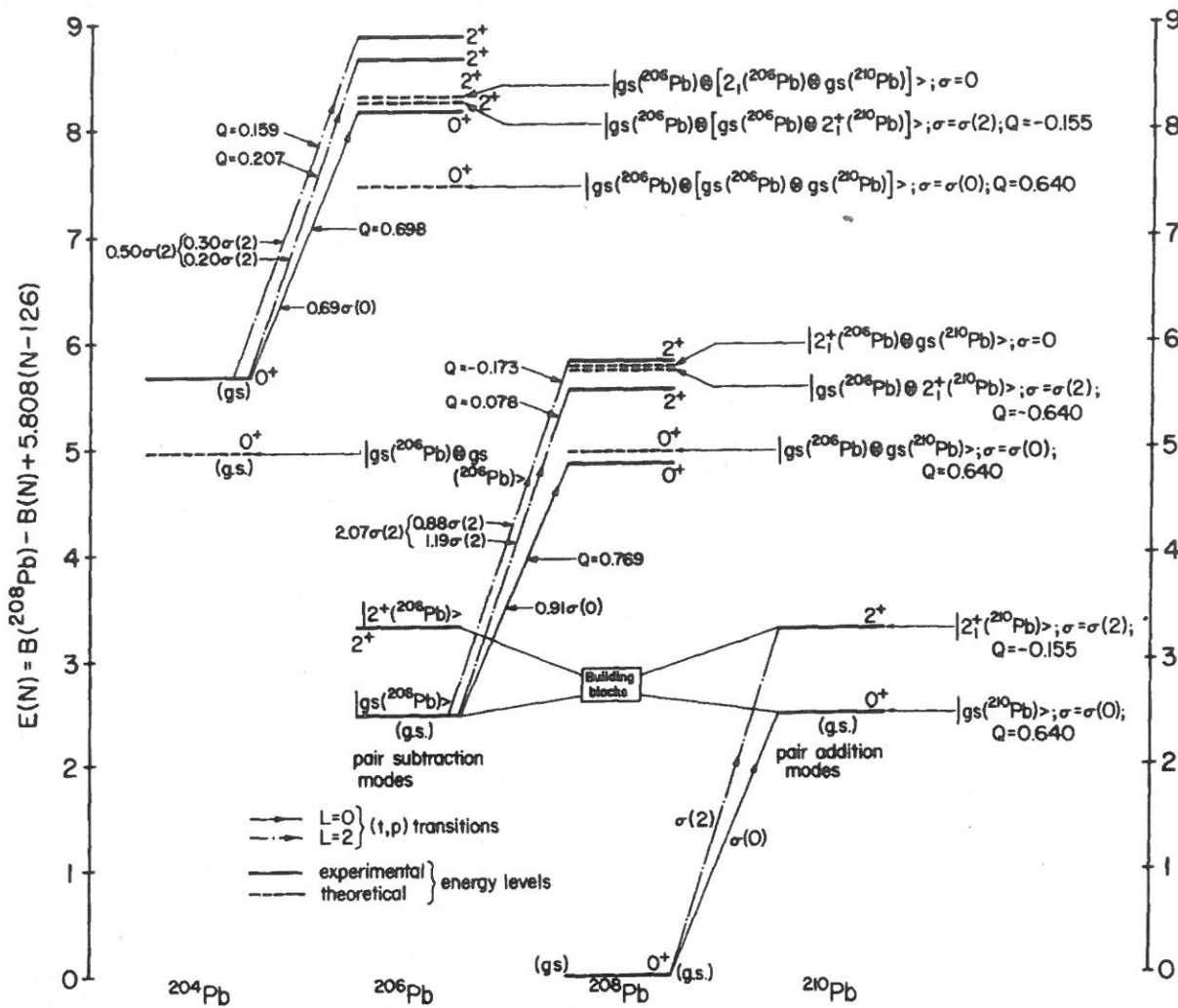


Fig. 1. Theoretical predictions of the pairing vibrational model for the $J^\pi = 0^+$ and 2^+ excited states of ^{208}Pb and ^{206}Pb expected to display the same Q -value, angular distribution and intensities in the $^{206}, ^{204}\text{Pb}$ (t, p) reactions as the ground state and first excited 2^+ state of ^{210}Pb in the ^{208}Pb (t, p) ^{210}Pb reaction.

These levels are depicted as dotted lines and their structure in terms of the pair addition and pair subtraction phonons (building blocks) are explicitly given.

The corresponding cross section and Q -values expected for each transition are also quoted for each state. The experimental energies (solid lines) and (t, p) cross sections are also given. In this case, the levels are joined by a continuous line ($L = 0$ transitions) or by a dotted line ($L = 2$ transitions) and the corresponding intensities in terms of the cross sections $\sigma(0) = \sigma(^{208}\text{Pb} (t, p) ^{210}\text{Pb} (\text{gs}))$ and $\sigma(2) = \sigma(^{208}\text{Pb} (t, p) ^{210}\text{Pb} (2^+))$ are given. Also quoted are the observed Q -values.

The experimental energy of the different ground states is given relative to the ^{208}Pb ground state and corrected by a linear function of the number of neutrons outside (or missing from) the $N = 126$ closed shell such that $E(^{206}\text{Pb} (\text{gs})) = E(^{210}\text{Pb} (\text{gs}))$. The corresponding expression [6] is $E_{\text{exp}}(N, Z = 82) = B(^{208}\text{Pb}) - B(N, Z = 82) + 5.808(N-126)$, where $B(N, Z)$ is the binding energy of the nucleus $A = N + Z$. Note that $\hbar\omega(0) = E_{\text{theor}}(^{206}\text{Pb} (\text{gs})) = E_{\text{theor}}(^{210}\text{Pb} (\text{gs})) = E_{\text{exp}}(^{206}\text{Pb} (\text{gs})) = E_{\text{exp}}(^{210}\text{Pb} (\text{gs})) = 2.493$ MeV, that $E_{\text{theor}}(^{206}\text{Pb} (2^+)) = E_{\text{exp}}(^{206}\text{Pb} (2^+)) = 3.294$ MeV and $E_{\text{theor}}(^{210}\text{Pb} (2^+)) = E_{\text{exp}}(^{210}\text{Pb} (2^+)) = 3.288$ MeV. The theoretical energy of any other state, for example of the 2^+ state $|gs(^{206}\text{Pb}) \otimes 2(^{210}\text{Pb}); 2^+\rangle$ of ^{206}Pb is equal to $2.493 + 3.294 + 2.493 = 8.280$ MeV (as measured from $^{208}\text{Pb} (\text{gs})$).

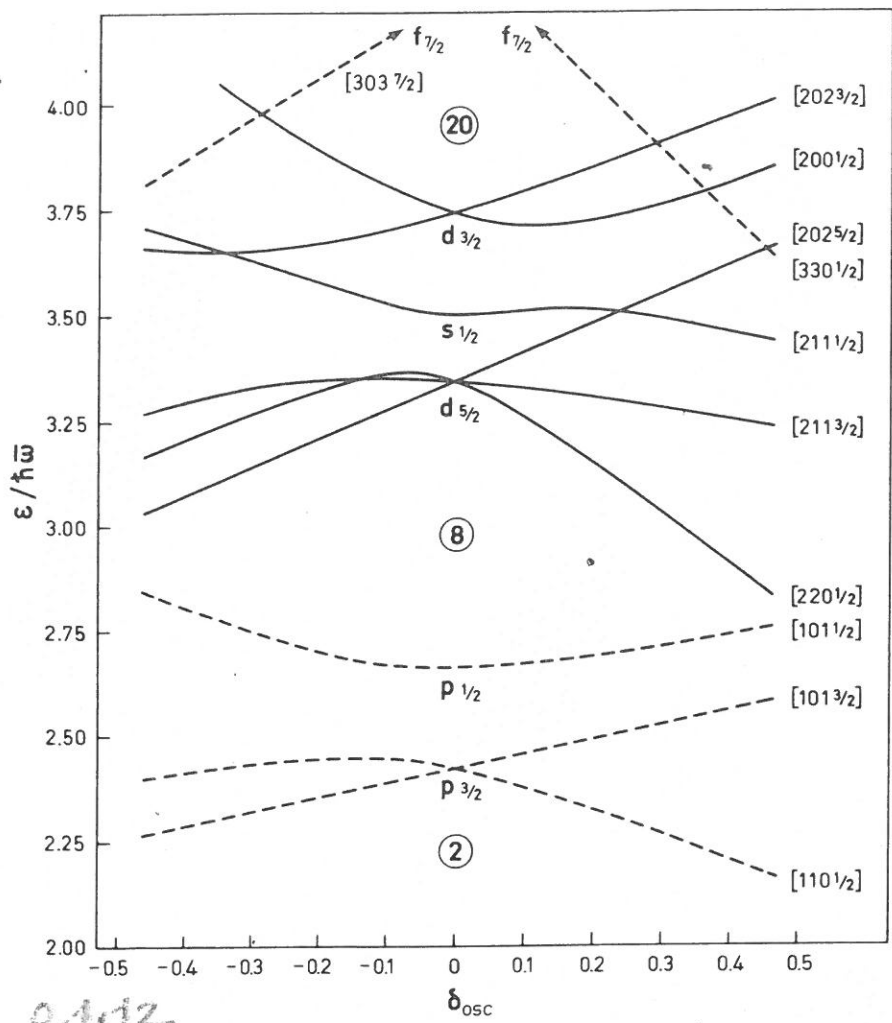


Figure 5-1 Spectrum of single-particle orbits in spheroidal potential (N and $Z < 20$). The spectrum is taken from B. R. Mottelson and S. G. Nilsson, *Mat. Fys. Skr. Dan. Vid. Selsk.* 1, no. 8 (1959). The orbits are labeled by the asymptotic quantum numbers $[Nn_3\Lambda\Omega]$ referring to large prolate deformations. Levels with even and odd parity are drawn with solid and dashed lines, respectively. *(after Bohr and Mottelson (1975))*

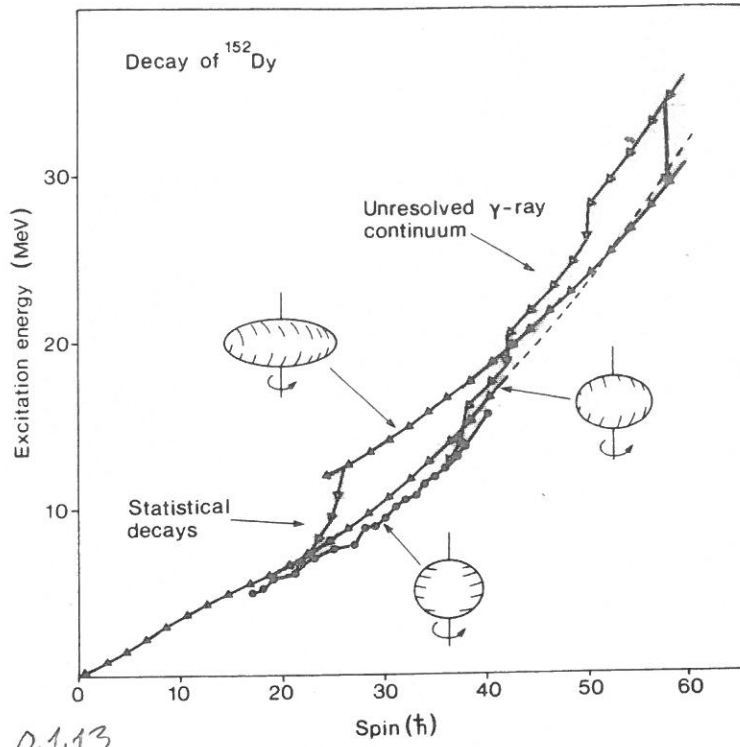


Figure 8 A schematic of the proposed γ -ray decay paths from a high-spin entry point in ^{152}Dy . The major initial decay flow occurs mainly via E2 transitions in the unresolved γ -ray continuum and reaches the oblate yrast structures between $30\hbar$ and $40\hbar$. A small 1% branch feeds the superdeformed band, which is assumed to become yrast at a spin of $50\text{--}55\hbar$. The deexcitation of the superdeformed band around $26\hbar$ occurs when the band is 3–5 MeV above yrast, and a statistical type of decay flow takes it into the oblate states between $19\hbar$ and $25\hbar$. The diagram also shows the low deformation prolate band (After Nolan and Twin (1988)).

P.J. Nolan and P.Twin, Superdeformed charge at high angular momentum, Ann. Rev. Nucl. and Particle Science, 38, 533 (1988)

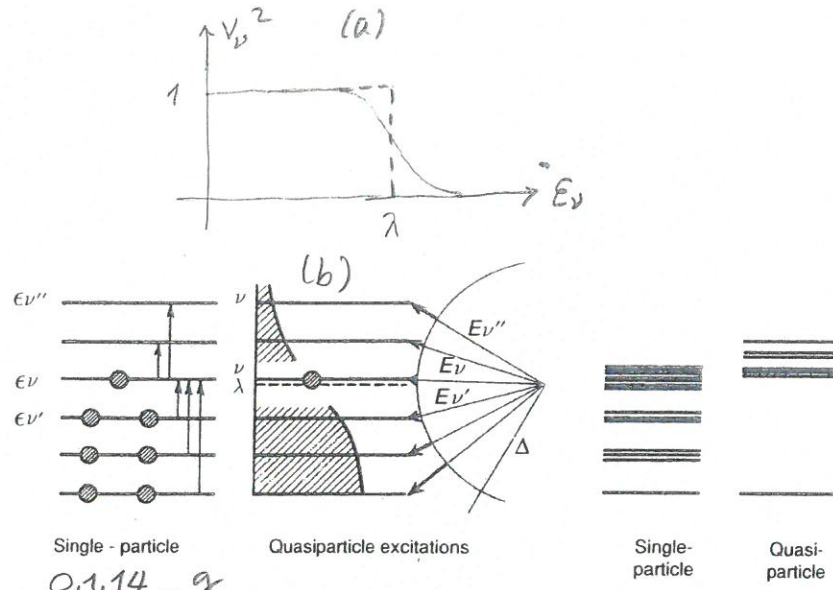
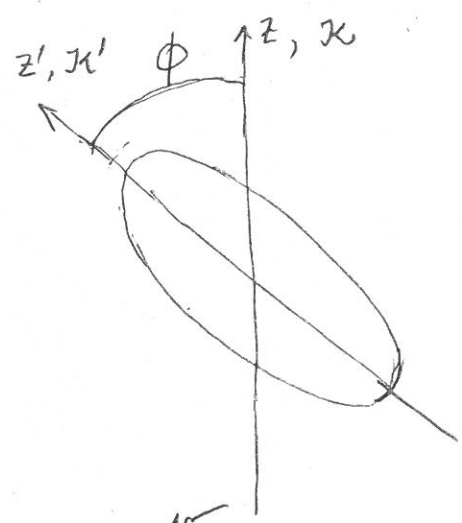


Figure 19. Ground state and excited states in the extreme independent single-particle model and in the pairing-correlated, superfluid model in the case of a system with an odd number of particles. In the first case, the energy of the ground state of the odd system differs from that of the even with one particle fewer by the energy difference $\varepsilon_v - \varepsilon_{v'}$, while in the second case by the energy $E_v = \sqrt{(\varepsilon_v - \lambda)^2 + \Delta^2} \approx \Delta$, associated with the fact the odd particle has no partner. Excited states can be obtained in the independent particle case by promoting the odd particle to states above the level ε_v , or by exciting one particle from the state below to the state ε_v or to one above it. To the left only a selected number of these excitations are shown. In the superfluid case excited states can be obtained by breaking of pairs in any orbit. The associated quasiparticle energy is drawn also here by an arrow of which the thin part indicates the contribution of the pairing gap and the thick part indicates the kinetic energy contribution, i.e. the contribution arising from the single-particle motion. Note the very different density of levels emerging from these two pictures, which are shown at the far left of the figure (after Nathan and Nilsson (1965)). Reprinted from *Alpha- Beta- and Gamma-Ray Spectroscopy*, Vol. 1, Nathan, H. and Nilsson, S. G., Editor Siegbahn, H., page 601, Copyright 1965, with permission from Elsevier.

(a) Independent (dashed line) and BCS occupation numbers; (b)



15
Fig. O.1.14

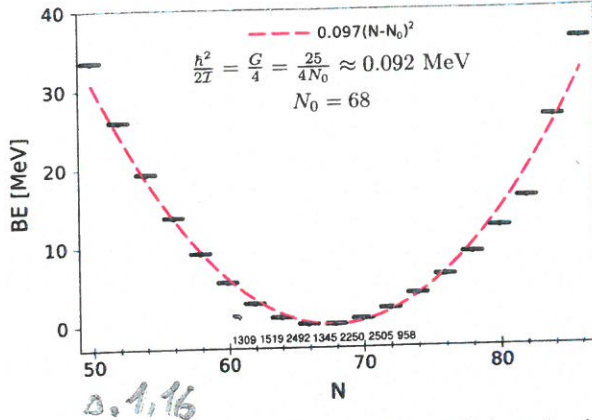


FIG. 9. (Color online) Pairing rotational band along the tin isotopes. The lines represent the energies calculated according to the expression $BE = B(^{50+N}\text{Sn}_N) - 8.124N + 46.33$ [10], subtracting the contribution of the single nucleon addition to the nuclear binding energy obtained by a linear fitting of the binding energies of the whole Sn chain. The estimate of $\hbar^2/2I$ was obtained using the single j -shell model (see, e.g., Ref. [10], Appendix II). The numbers given on the abscissa are the absolute value of the experimental $gs \rightarrow gs$ cross section (in units of μb , see Table IV).

Bibliography

- J. Bardeen, L. N. Cooper, and J. R. Schrieffer. Microscopic theory of superconductivity. *Physical Review*, 106:162, 1957a.
- J. Bardeen, L. N. Cooper, and J. R. Schrieffer. Theory of superconductivity. *Physical Review*, 108:1175, 1957b.
- F. Barranco, R. A. Broglia, G. Colò, G. Gori, E. Vigezzi, and P. F. Bortignon. Many-body effects in nuclear structure. *European Physical Journal A*, 21:57, 2004.
- A. Bohr and B. R. Mottelson. *Nuclear Structure, Vol.I*. Benjamin, New York, 1969.
- A. Bohr, B. R. Mottelson, and D. Pines. Possible analogy between the excitation spectra of nuclei and those of the superconducting metallic state. *Physical Review*, 110:936, 1958.
- N. Bohr and J. A. Wheeler. The mechanism of nuclear fission. *Phys. Rev.*, 56:426, 1939.
- Bohr, A. and B. R. Mottelson. *Nuclear Structure, Vol.II*. Benjamin, New York, 1975.
- P. A. M. Dirac. *The principles of quantum mechanics*. Oxford University Press, London, 1930.
- W. Elsasser. Sur le principe de Pauli dans les noyaux. *J. Phys. Radium*, 4:549, 1933.
- O. Haxel, J. H. D. Jensen, and H. E. Suess. On the “Magic Numbers” in nuclear structure. *Phys. Rev.*, 75:1766, 1949.
- M. Mayer and J. Jensen. *Elementary Theory of Nuclear Structure*. Wiley, New York, NY, 1955.
- M. G. Mayer. On closed shells in nuclei. *Phys. Rev.*, 74:235, 1948.
- M. G. Mayer. On closed shells in nuclei. ii. *Phys. Rev.*, 75:1969, 1949.
- M. G. Mayer. The shell model. *Nobel Lecture*, 1963.

BIBLIOGRAPHY

- M. G. Mayer and E. Teller. On the origin of elements. *Phys. Rev.*, 76:1226, 1949.
- L. Meitner and O. R. Frisch. Products of the fission of the uranium nucleus. *Nature*, 143:239, 1939.
- C. F. Weizsäcker. *Z. Phys.*, 96:431, 1935.